Eur. Phys. J. B **53**, 213–217 (2006)
DOI: 10.1140/epjb/e2006-00371-x

THE EUROPEAN PHYSICAL JOURNAL B

Electronic structure and magnetism of YbRhSn

T. Jeong[a]

DPMC, University of Geneva, 24 Quai Ernest-Ansermet, CH-1211 Geneva 4, Switzerland

Received 13 July 2006 / Received in final form 1st September 2006
Published online 13 October 2006 –

Abstract. The electronic band structure of YbRhSn has been calculated using the self-consistent full potential nonorthogonal local orbital minimum basis scheme based on the density functional theory. We investigated the electronic structure with the spin-orbit interaction and on-site Coulomb potential for the Yb-derived $4f$ orbitals to obtain the correct ground state of YbRhSn. The exchange interaction between local f electrons and conduction electrons play an important role in the heavy fermion characters of them. The fully relativistic band structure scheme shows that spin-orbit coupling splits the $4f$ states into two manifolds, the $4f_{7/2}$ and the $4f_{5/2}$ multiplet.

PACS. 71.10.Hf Non-Fermi-liquid ground states, electron phase diagrams and phase transitions in model systems – 71.18.+y Fermi surface: calculations and measurements; effective mass, g factor – 72.20.Eh – 75.30.Mb Valence fluctuation, Kondo lattice, and heavy-fermion phenomena

1 Introduction

The Ce- and Yb-based heavy fermion systems have been attractive in condensed matter physics in recent years [1]. The characteristics of the unusual phenomena of heavy fermions is a large electronic specific heat at low temperatures, or equivalently to an effective electron mass of 10^2–10^3 that of the free-electron mass. These systems typically have a large Pauli susceptibility at low T as a consequence of the large density of states. The temperature dependence of C and χ can be explained in terms of narrow resonant levels or a narrow bandwidth with a typical width of 1 meV or so. The narrow peak in the density of states has been attributed to the Kondo effect, but its formation is still unknown. In stoichiometric heavy-fermion compounds the resistivity initially increases as one lowers the temperature T, then goes through a large maximum and shows a sharp decrease at very low T. Both features, the existence of a maximum and the high resistivity at this maximum, are uncommon to normal metals. The rapid decrease of the resistivity at low temperature is caused by a transition from incoherent to coherent scattering of the conduction electrons by the rare-earth ions [2].

The magnetic susceptibility of YbRhSn follows the Curie-Weiss law at high temperature with an effective moment of 4.4 μ_B, and a Curie-Weiss temperature $\Theta = -20$ K [3]. The resistivity $\rho(T)$ of YbRhSn diminishes almost linearly as T decreases. Below 10 K, a weak logarithmic increase is followed by a maximum at $T_{max,\rho} \sim 4.5$ K. Two magnetic transitions are present at 1.85 K and 1.4 K. The transport properties of YbRhSn resemble the characteristic features observed in several Ce-based Kondo lattices, namely the presence of Kondo effect in $\rho(T)$ and enhanced values of the thermoelectric power(TEP) like in $CeCu_2Ge_2$ [4]. The resistivity $\rho(T)$ data of YbRhSn show broad anomaly at ∼150 K which are due to the interaction of Kondo-type incoherent scattering on excited crystal electric field(CEF) levels [5]. At lower temperatures the $\rho(T) \propto -\ln T$ dependence, present in different degree of intensity in YbRhSn and followed by a clear maximum at $T_{max,\rho}$, signals the effect of incoherence Kondo scattering on the ground state doublet. The value of $T_{max,\rho}$ agrees with the value of the Kondo temperature extracted from the scaling behavior of the magnetoresistivity data. Kaczorowski et al. studied electronic structure of ternary YbTX compounds (T = transition metal, M = Sn, Bi) by X-ray photoemission spectroscopy(XPS) [7,8]. Their electronic structure studies show that the valence bands are formed mainly by the $4f$ orbitals of Y and the $4d$ orbitals of Rh. Their XPS experimental results indicate that the Y ion is trivalent and the electrical behavior is characteristic of dense Kondo systems, and the low temperature specific heat data indicate a possible heavy fermion ground state.

In order to understand the electronic and magnetic properties of YbRhSn, we need the electronic band structure studies based on the density functional theory. In this work, the precise self-consistent full potential local orbital

[a] e-mail: tjeong57@hotmail.com

minimum basis band structure scheme (FPLO) are employed to investigate the electronic and magnetic properties of YbRhSn with LDA, LDA+U and fully relativistic schemes.

2 Crystal structure and method of calculations

YbRhSn crystallizes in the hexagonal structure which belongs to the $P\bar{6}2m$ space group, with Yb occupying the 3g site, Rh the 3f and Sn the 1b and 2c sites. We used experimental lattice constants, $a = 6.925$ Åand $c = 3.984$ Å, in the calculation described below. There are three formula units in the primitive cell.

We have applied the full-potential nonorthogonal local-orbital minimum-basis (FPLO) scheme within the local density approximation (LDA) [6]. In these scalar relativistic calculations we used the exchange and correlation potential of Perdew and Wang [9]. Yb $6s, 6p, 5d$, Rh $5s, 5p, 4d$ and Sn $5s, 5p, 4d$ states were included as valence states. We included the relatively extended semicore $4s, 4p, 4d, 4f, 5s, 5p$ states of Yb and $4s, 4p$ states of Rh and $4s, 4p$ states of Sn as band states because of the considerable overlap of these states on nearest neighbors. This overlap would be otherwise neglected in our FPLO scheme. Other lower states were treated as core states. Yb 6p states were added to increase the quality of the basis set. The spatial extension of the basis orbitals, controlled by a confining potential $(r/r_0)^4$, was optimized to minimize the total energy. The self-consistent potentials were carried out on a k mesh of 12 k points in each direction of the Brillouin zone, which corresponds to 343 k points in the irreducible zone. A careful sampling of the Brillouin zone is necessitated by the fine structures in the density of states near Fermi level E_F.

3 Results and discussion

We first show the full non-magnetic band structures of YbRhSn within LDA scheme in Figure 1. The Sn $5s$ bands lie between -10 eV and -8 eV. Above them there are Rh $5p$ characters around -5 eV. Between -3 eV and -0.5 eV there are of mixed Rh $5p$ and Sn $3p$ states. Those very flat bands below the Fermi level are mainly the Yb-centered $4f$ characters. A prominent feature of the band structure near E_F, besides the $4f$ bands, is the Yb $5d$ character which hybridizes with the Yb $4f$ bands. Above the Fermi energy there are varying amount of Yb $6s, 5d$. We also study the on-site atomic-like correlation effects beyond LDA by using LDA+U approach in a rotationally invariant, full potential implementation [10]. Minimizing the LDA+U total energy functional with spin-orbit coupling(SOC) treated self-consistently [11] generates not only the ground state energy and spin densities, but also effective one-electron states and energies that provides the orbital contribution to the moment and Fermi surfaces. The basic difference of

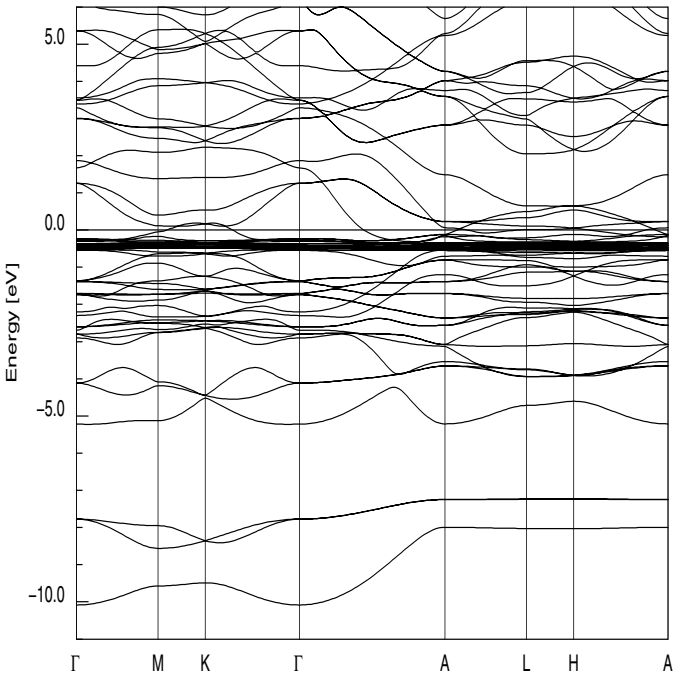

Fig. 1. The full LDA non-magnetic band structure of YbRhSn along the symmetry lines. The Fermi level is located at 0.0 in in the figure.

LDA+U calculations from the LDA is its explicit dependence on the on-site spin and orbitally resolved occupation matrices. The Coulomb potential U and the exchange coupling J for the Yb 4f orbitals have been chosen to be 7.0 and 0.68 eV respectively. The resulting band structure calculated within the LDA+U scheme is shown in middle panel of Figure 2. We observe that the crystal field splittings of Yb 4f bands within LDA are quite small and in fact difficult to identify due to hybridization with itinerant bands. From LDA+U, the 4f bands are still very flat but are split into five manifolds (at -3.2 eV, -2.5 eV, -1.0 eV, -0.5 eV and $+1.2$ eV) by some combination of the crystal field and the anisotropy of the U interaction. When we choose Coulomb potential U with the value of 5.0, the three manifolds are located at -2.6, -1.8, -0.7, -0.3, and $+0.7$ eV. We also calculated fully relativistic band structure to see the spin-orbit coupling effects, which is shown in the bottom panel of Figure 2. As expected spin-orbit coupling splits the 4f states into two manifolds, located 0.1 eV and 1.4 eV below the Fermi level, the $4f_{7/2}$ and the $4f_{5/2}$ multiplet respectively. At this point, it would be elucidating to see the total count of f electrons in each calculation schemes. Our calculation shows that the number of f electrons is 13.9 in LDA, 13.5 in LDA+SOC(fully relativistic), 13.1 in LDA+U.

The atom and symmetry projected densities of states (DOS) shown in Figure 3 clarify the characters of the bands. Because only the DOS distribution near the Fermi level determines the magnetic properties, we concentrate our attention upon the DOS in the vicinity of the Fermi level. At this range, the valence states for Yb or Rh atoms are dominated by $4f$ and $4d$ electrons respectively.

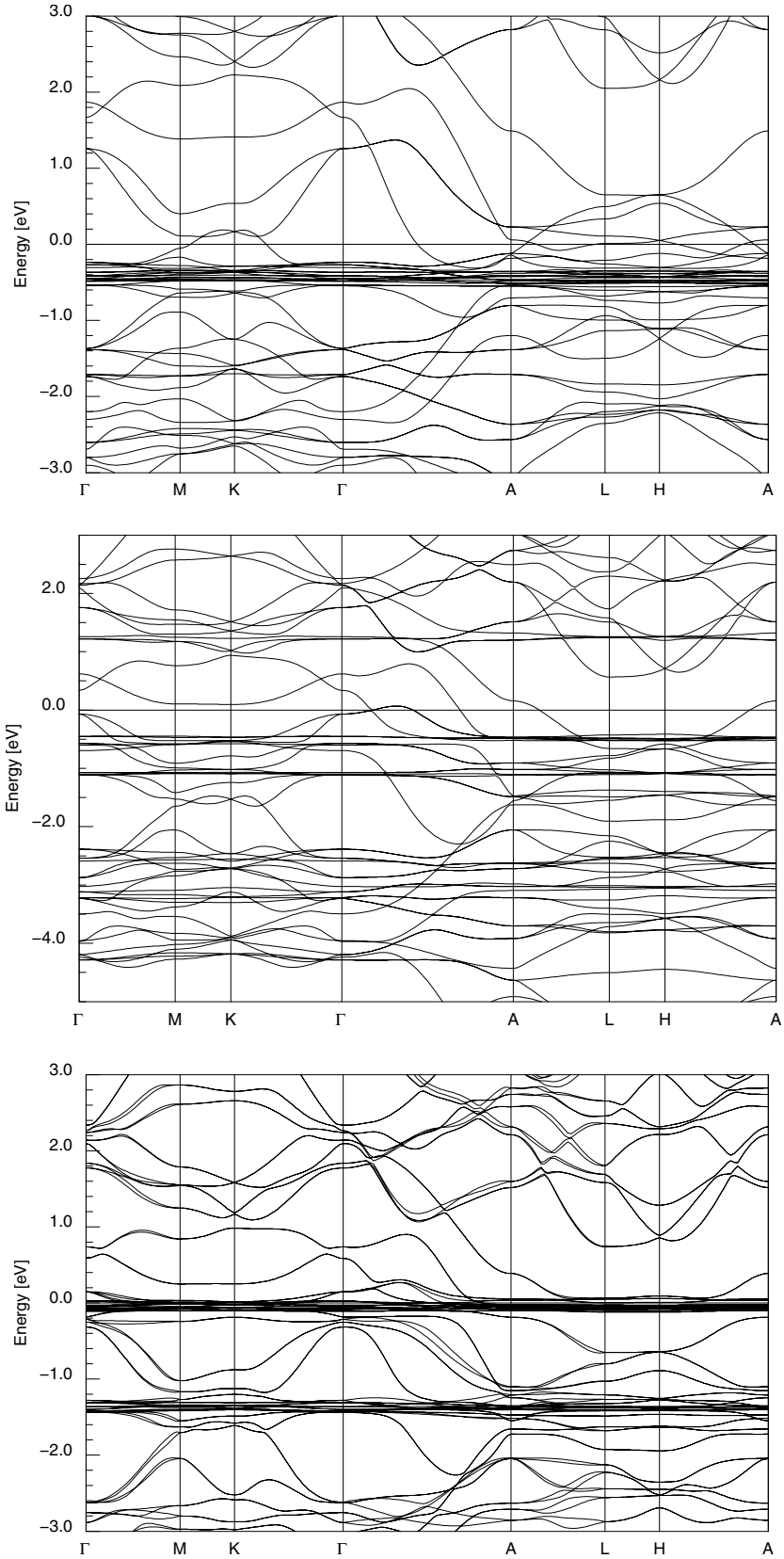

Fig. 2. The non-magnetic band structure near the Fermi level with three different schemes. Top panel: the LDA band structure of YbRhSn along symmetry lines. The very flat bands near the Fermi level are the Yb 4f bands. Middle panel: the band structure within the LDA+U scheme showing that the 4f bands split into five manifolds. Bottom panel: the fully relativistic band structure of YbRhSn showing that spin-orbit coupling splits the 4f states into two manifolds.

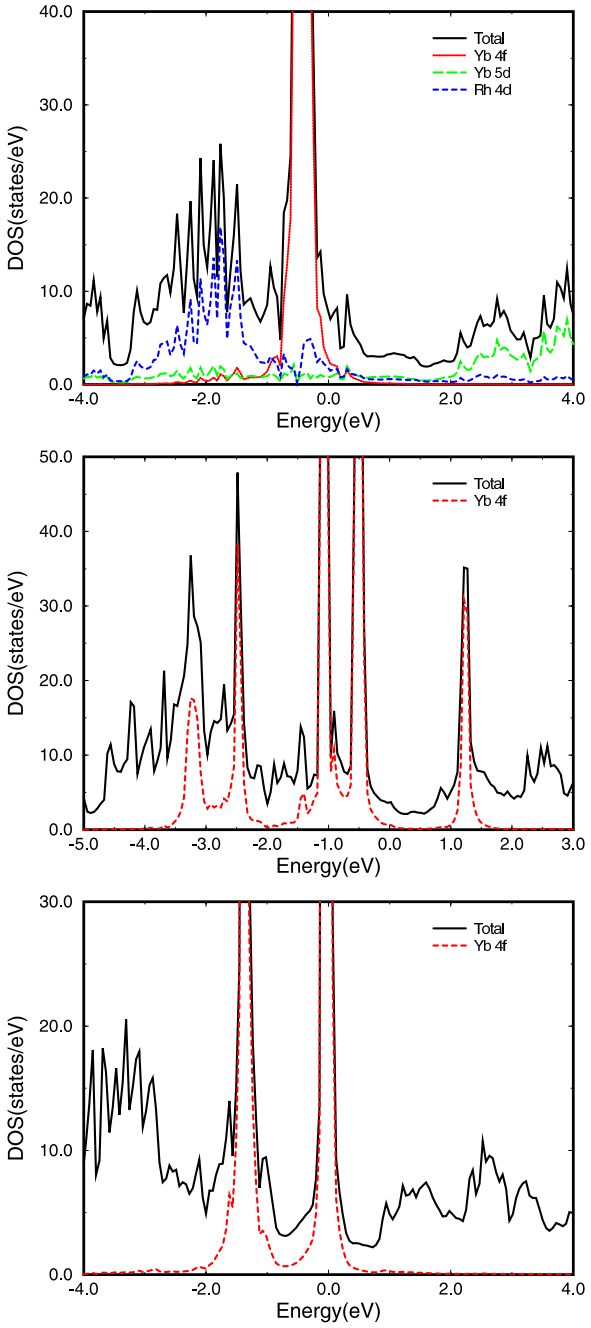

Fig. 3. The non-magnetic density of states of YbRhSn. Top panel: DOS of LDA, the Yb 4f bands dominate the states near the Fermi level. Middle panel: DOS of LDA+U, the 4f bands split into five manifolds. Bottom panel: Showing the spin-orbit coupling effects of fully relativistic calculation. The splitting is about 1.3 eV.

From Figure 3, it can be found that within the LDA calculation, the DOS at the Fermi level are mainly of Yb-derived $4f$ states. When the spin-orbital coupling along the axis (0 0 1) is taken into account, the $4f$ orbitals are slightly modified. The spin 4f states become wider and the energy shift between centers becomes larger. This is due to the partial splitting between the degenerate $4f$ states.

We also studied for the spin polarized band structure for YbRhSn. Band calculation with the LDA framework cannot yield correctly magnetic moment for many Yb compounds because of the strong correlation interaction between f orbitals. The spin-orbit interaction in these systems is sometimes large and the orbital contribution to magnetic moment cannot be neglected. The calculated magnetic moment of YbRhSn within LDA scheme is 1.61 μ_B per formular unit, it is mainly from the Yb-derived 4f orbitals. When the on-site correlation potential is added to the Yb 4f electron, the degeneracy between the different f orbits would be lifted and the Hund's rules dominate the locally occupied 4f electrons, which yields the total magnetic moment 1.54 μ_B/cell. With fully relativistic scheme we calculated the magnetic moment of the value 1.56μ_B/cell. The experimental magnetic moment of YbRhSn is 4.4 μ_B which is bigger than the calculated values [3].

In the following we study the uniform magnetic susceptibility using the method of Janak [14]. The uniform magnetic susceptibility of a metal can be written as

$$\chi = \frac{\chi_0}{1 - N(E_F)I}, \tag{1}$$

where the numerator stands for the Pauli susceptibility of a gas of non-interacting electrons proportional to the density of states at the Fermi level $N(E_F)$, and the denominator represents the enhancement due to electron-electron interaction. Within the Kohn-Sham formalism of density functional theory the Stoner parameter I is related to the second derivative of the exchange-correlation functional with respect to the magnetization density. We have evaluated, within the density functional theory formalism, the Stoner enhancement of the susceptibility $\chi = \frac{\chi_0}{1-IN(E_F)} \equiv S\chi_0$, where $\chi_0 = 2\mu_B^2 N(E_F)$ is the non-interacting susceptibility and S gives the electron-electron enhancement in terms of the Stoner constant I. We have calculated I using both the Janak-Vosko-Perdew theory [14] and fixed spin moment calculations [15]. The calculated density of states $N(E_F) = 3.67\,\mathrm{eV}^{-1}$ and Stoner parameter $I = 0.33$ gives $IN(E_F) = 1.22$, larger than unity, corresponding to a ferromagnetic instability. In this calculation we used $N(E_F)$ of LDA scheme.

Heavy fermion compound is characterized by a larger electronic specific heat coefficient γ. YbRhSn is a heavy fermion compound with $\gamma = 360$ mJ/K^{2}mol. The large specific heat coefficient of YbRhSn compound could not be yielded by our band calculation. This can be seen from the calculated electronic structure. It can be found that the total number of DOS at the Fermi level is about 3.67 states/eV, which corresponds $\gamma_b = 8.57$ mJ/K^{2}mol and underestimate the experiment value by a factor of 42.0. The discrepancy between the band calculation and experiment for specific heat coefficient is attributed to the formation of quasiparticle. There is exchange interaction J between the local f and the conduction electrons in YbRhSn. The ground state of Yb compound is determined by the competition of the Kondo and indirect RKKY interaction. With a large J, the Kondo coupling

becomes strong and the system located at the borderline of magnetic-nonmagnetic transition. The exchanging interaction between the local f electron and the conduction electrons will result in the formation of quasiparticle. It has a larger mass compared with bare electron and the enhancement of mass increases with the increase of exchanging. Because of the volume contraction, the exchange interaction between the f and the conduction electrons is large in YbRhSn. This will result in the f electrons to behave like itinerant electrons and the narrow f bands to be located at the Fermi level. On the other hand, when the exchanging interaction between f and conduction electrons is smaller, the occupied 4f orbitals are located near the Fermi level while the unoccupied 4f orbitals are at the conduction bands. The quasiparticle mass is appropriate to the number of DOS at the Fermi level. So the quasiparticle mass is largely enhanced in YbRhSn. Indeed, it has been shown that when the Yb 4f electrons in YbRhSn are treated as localized electrons, the quasiparticle mass was only enhanced over the band calculation by a factor 42.0.

At this point we need to discuss a remained question: which band structure(LDA, LDA+U or LDA+SOC) is more realistic? In LDA+SOC(the fully relativistic scheme), SOC is applied at the one-electron level, that is, each $4f$ orbital acquires its own $j = l \pm s(\frac{7}{2}$ or$\frac{7}{2})$ label and character. In LDA+U, one can follow Hund's rules to some extent: maximize $S = \Sigma_i s_i$, and maximize $L = \Sigma_i l_i$, and study various values of J(or even of L). The LDA+U method has proven to be a fruitful approach in the model calculations of the bulk and surface electronic structure of Gd[12] and other rare earth system[13]. On the other hand, $4f$ single particle-like excitations are likely to be characterized by the $\frac{7}{2}, \frac{5}{2}$ labels. The excitations $f^0 \rightarrow f^1$ or $f^{14} \rightarrow f^{13}$ are likely to show SOC aspects directly. Therefore further experimental investigations, such as Angle-resolved photoemission spectroscopy technique(a powerful technique to directly probe the electronic structure of solids) should be quite interesting.

4 Summary

In this work we studied the electronic band structure with three different schemes. It shows that the Coulomb potential on Yb $4f$ orbitals and spin-orbit interaction is a key factor to understand the electronic and magnetic properties of YbRhSn. When the Coulomb potential is added to the Yb 4f orbitals, the degeneracy between the different f orbits would be lifted and they are split into lower Hubbard bands and upper Hubbard bands. The exchange interaction between local f electrons and conduction electrons play an important role in the heavy fermion characters of them. And the fully relativistic band structure scheme shows that spin-orbit coupling splits the 4f states into two manifolds, the $4f_{7/2}$ and the $4f_{5/2}$ multiplet. The f-electrons can be delocalized through the hybridization with conduction electrons. If there exists no hybridization between f and conduction electrons, the f-electron number becomes just an integer and the f-electrons are localized. The almost localized f-electrons and delocalized conduction electrons hybridize to deviate the f-electron number from an integer, and keep the metallic state against the strong electron correlation between f-electrons. Therefore the hybridization between f and conduction d electrons plays a important role in YbRhSn.

References

1. G.R. Stewart, Rev. Mod. Phys. **73**, 797 (2001)
2. P.A. Lee, T.M. Rice, J.W. Serene, L.Y. Sham, J.W. Wilkins, Comments Condens. Matter Phys. **12**, 99 (1986)
3. O. Trovarelli, C. Geibel, R. Cardsoso, S. Mederle, R. Borth, B. Buschinger, F.M. Grosche, Y. Grin, G. Sparn, F. Steglich, Phys. Rev. B. **61**, 9467 (2000)
4. N. Grewe, F. Steglich, in *Handbook on the Physics and Chemistry of the Rare Earths*, edited by K.A.Gschneider Jr., L. Eyring (North-Holland, Amsterdam, 1991), Vol. 14, p. 343
5. D. Cornut, B. Coqblin, Phys. Rev. B **5**, 4541 (1972)
6. K. Koepernik, H. Eschrig, Phys. Rev. B **59**, 1743 (1999); H. Eschrig, *Optimized LCAO Method and the electronic Structure of Extended Systems* (Springer, Berlin, 1989)
7. D. Kaczorowski, A. Leithe-Jasper, P. Rogl, H. Flandorfer, T. Cichorek, R. Pietri, B. Andraka Phys. Rev. B. **60**, 422 (1999)
8. A. Szytula, A. Jezierski, B. Penc, A. Winiarski, A. Leithe-Jasper, D. Kaczorowski, J. Alloys. Compounds **360**, 42 (2003)
9. J.P. Perdew, Y. Wang, Phys. Rev. B **45**, 13244 (1992)
10. A.I. Liechtenstein, V.I. Anisimov, J. Zaanen, Phys. Rev. B **52**, R5468 (1995)
11. A.B. Shick, D.L. Novikov, A.J. Freeman, Phys. Rev. B **57**, R14259 (1997)
12. A.B. Schik, W.E. Pickett, C.S. Fadley, J. Appl. Phys. **87**, 5878 (2000)
13. J. Kunes, W. Ku, W.E. Pickett, J. Phys. Soc. Jpn **74**, 1408 (2005)
14. J.F. Janak, Phys. Rev. B **16**, 255 (1977); S.H. Vosko, J.P. Perdew, Can. J. Phys. **53**, 1385 (1975)
15. K. Schwarz, P. Mohn, J. Phys. F **14**, L129 (1984)